

SI1. Addition of emergent OPs

As in Eq. (1) we write the position of atom i in subsystem S as

$$\vec{r}_i = \sum_k \bar{\Phi}_k U_{ki} + \bar{\sigma}_i, \quad (\text{SI1})$$

where $\bar{\sigma}_i$ denotes the residual displacement of atom i resulting from a finite truncation of the k sum. The residuals $\bar{\sigma}_i$, in turn, are expressed via a set of OP-like variables $\bar{\Phi}_{k,new}$, such that

$$\bar{\sigma}_i = \sum_{k,new} \bar{\Phi}_{k,new} U_{ki,new}, \quad (\text{SI2})$$

where indices k,new are not in the set of OPs and the polynomials $U_{ki,new} \equiv U_{k,new}(\vec{r}_i^0)$ are mass-weighted orthogonal to those for the $\bar{\Phi}_k$ that constitute the initial set of subsystem-centered OPs.

The mapping between OPs and atomic positions is 1:1 when the total number of $\bar{\Phi}_k$ and $\bar{\Phi}_{k,new}$ equals the number of atoms N in the system. Multiplying (SI1) by $U_{k'i,new}$, summing over all i , and using the orthogonality conditions we get

$$\bar{\Phi}_{k,new} = \frac{\sum_{i=1}^N m_i U_{ki,new} \bar{\sigma}_i}{\sum_{i=1}^N m_i \{U_{ki,new}\}^2}. \quad (\text{SI3})$$

Thus additional OPs are constructed from the population of growing residuals.

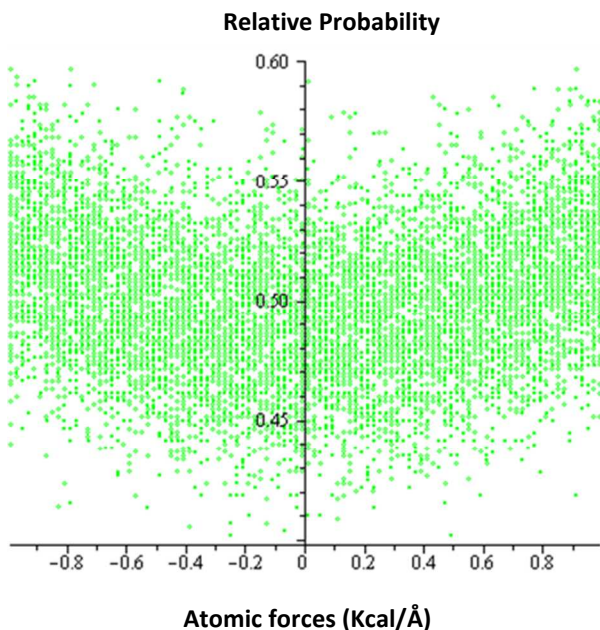


Fig. S1 Histogram of atomic forces (projected along the ray from the center of mass) for the expanding h4-truncated pentamer at 4 ns. Unlike the OP forces (Figs. 2(a)-(c)), histogram for atomic forces shows no clear trend in direction or magnitude.

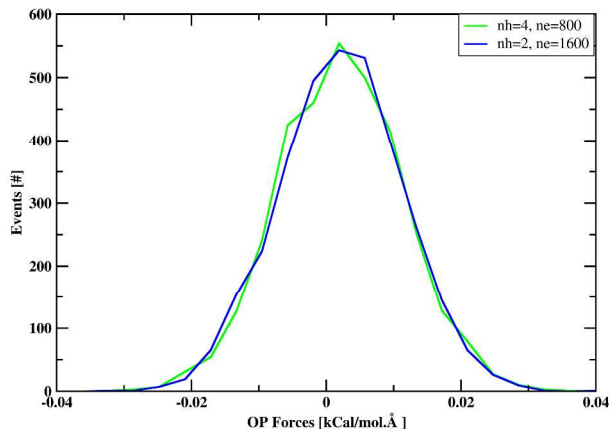


Fig. S2 Line histograms showing distribution of typical OP forces (here, f_k^m ; $k_1=1$, $k_2=0$ and $k_3=0$) for ensembles constructed using $N_h=4$, $N_e=800$ and $N_h=2$, $N_e=1600$. The distribution is in agreement with those from large non-history ensembles ($N_h=0$, $N_e=3200$) and other history enhanced ensembles ($N_h=8$, $N_e=400$) at the same time. Positively peaked distribution of these forces implies overall expansion of the pentamer.

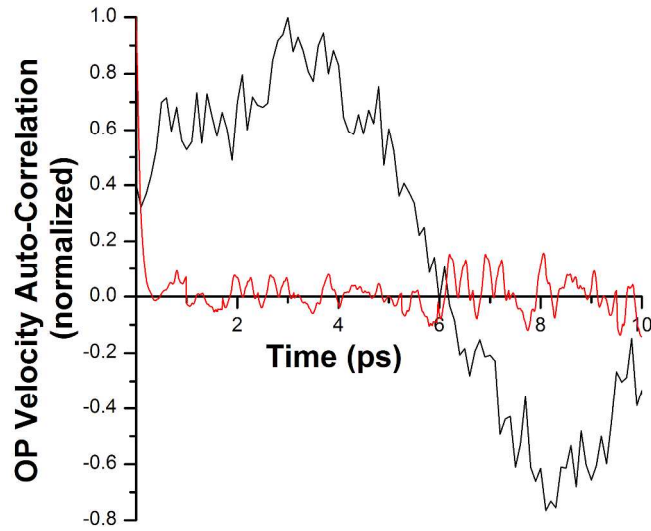


Fig. S3 Long-time tail appearing in the Φ_{001Z} velocity autocorrelation function of one pentamer in the absence of Φ_{100X} for the same. Also shown is the velocity autocorrelation decay in Φ_{001Z} when all coupled modes, i.e., $\bar{\Phi}_k$ for $\underline{k} = \{000, 100, 010, 001\}$ are incorporated as OPs (red).

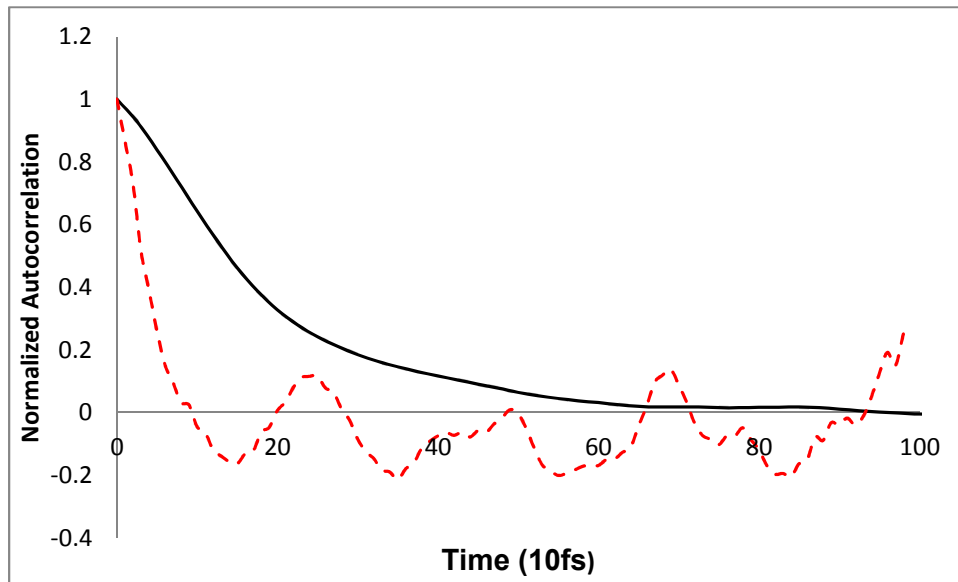


Fig. S4 The velocity autocorrelation function of a typical OP and the autocorrelation function of the associated force. These functions have correlation times well-separated and a Markovian behavior is expected.

Langevin timestep #

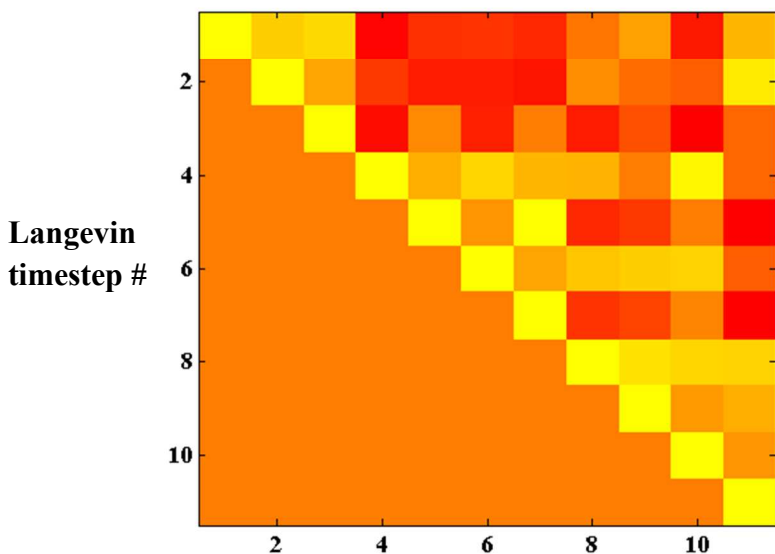


Fig. S5

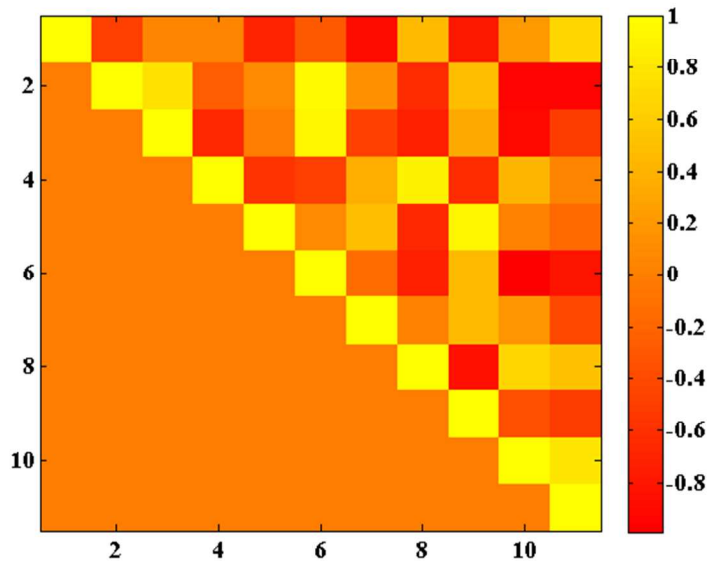


Fig.S6

Correlation between the thermal average forces obtained from constant OP ensembles of size 1600 and 200 every Langevin timestep (20ps), showing off-diagonal terms decrease as ensemble size decreases. This implies coherence in the thermal average forces over time decreases when ensembles used for averaging are incomplete.

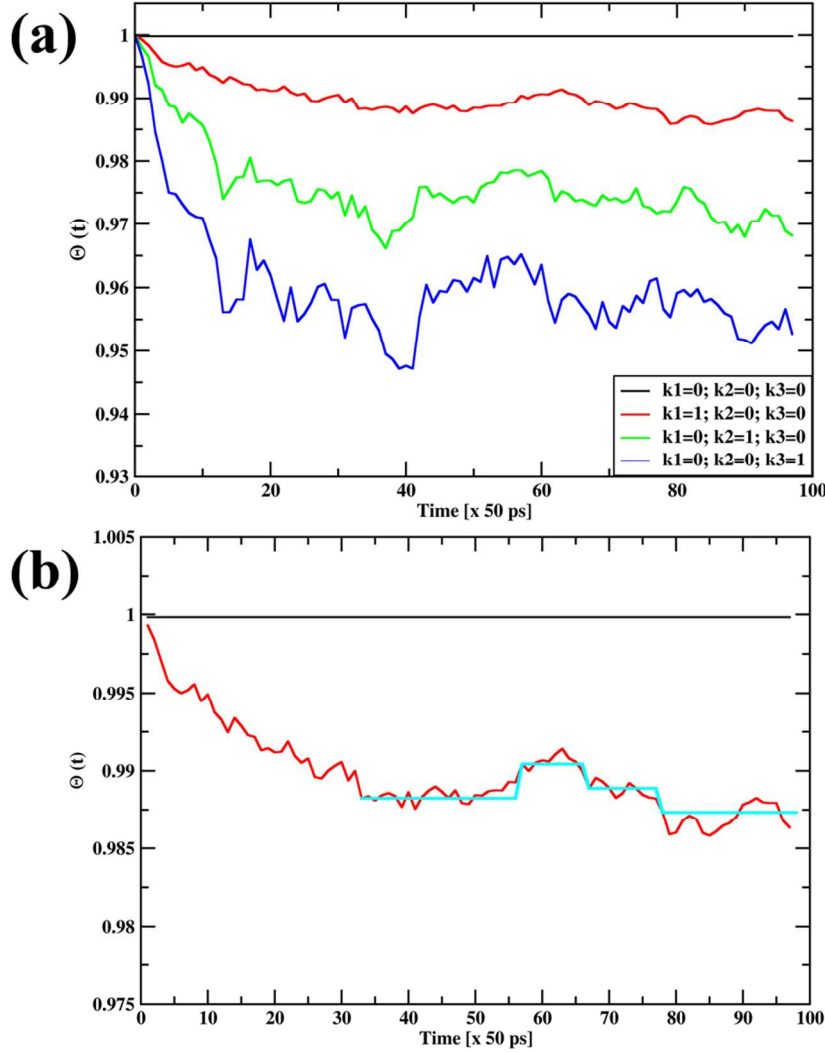


Fig. S7 (a) Evolution of $\Theta(t)$, cosine of the angle of rotation from the original basis vector

orientation at $t=0$ to that at time t , for typical $\bar{\Phi}_k$. We define, $\Theta_k(t) = \frac{\sum_{i=1}^N m_i U_{ki}(t) U_{ki}(0)}{\sum_{i=1}^N m_i \{U_{ki}(0)\}^2}$.

Deviation of $\Theta(t)$ from unity implies a change in the reference structure \bar{r}_i^0 as reflected in the dynamical U_{ki} . **(b)** The basis vectors U_{ki} (Eq. (1)) rotate slower than do the corresponding OPs (Fig. 4). Thus, U_{ki} can be held constant over a period of 0.6ns or more (blue line), i.e., thirty

20ps timesteps as Θ stays roughly constant over such interval. Every time the reference structure changes, polynomials are reconstructed in terms of the new reference and OPs are redefined.

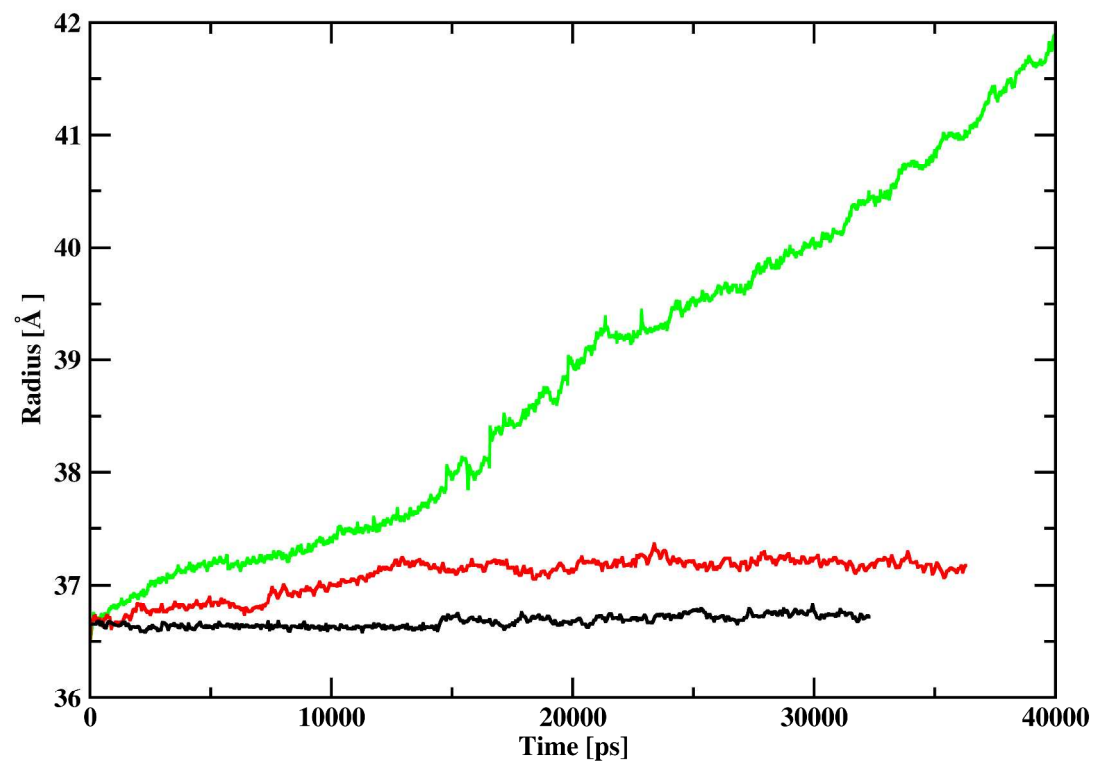


Fig S8 Changes in radius of gyration over time for a complete (black), h4-truncated (red), and h2,h3,h4-truncated HPV pentamer showing the first two structures initially expand and then remain stable, while the third expands more extensively.